

Application of atomic magnetometry in magnetic particle detection

S. Xu,^{a)} M. H. Donaldson, and A. Pines^{b)}

*Department of Chemistry, University of California at Berkeley, Berkeley, California 94720
and Materials Sciences Division, Lawrence Berkeley National Laboratory, Berkeley, California 94720*

S. M. Rochester and D. Budker^{c)}

*Department of Physics, University of California at Berkeley, Berkeley, California 94720
and Nuclear Sciences Division, Lawrence Berkeley National Laboratory Berkeley, California 94720*

V. V. Yashchuk

Advanced Light Source, Lawrence Berkeley National Laboratory, Berkeley, California 94720

(Received 15 September 2006; accepted 22 October 2006; published online 1 December 2006)

The authors demonstrate the detection of magnetic particles carried by water in a continuous flow using an atomic magnetic gradiometer. Studies on three types of magnetic particles are presented: a single cobalt particle (diameter $\sim 150 \mu\text{m}$, multidomain), a suspension of superparamagnetic magnetite particles (diameter $\sim 1 \mu\text{m}$), and ferromagnetic cobalt nanoparticles (diameter $\sim 10 \text{ nm}$). Estimated detection limits are $20 \mu\text{m}$ diameter for a single cobalt particle at a water flow rate of 30 ml/min , 5×10^3 magnetite particles at 160 ml/min , and 50 pl for the ferromagnetic fluid of cobalt nanoparticles at 130 ml/min . Possible applications of their method are discussed. © 2006 American Institute of Physics. [DOI: 10.1063/1.2400077]

Magnetic particles of micrometer and nanometer sizes are widely used in biomolecular labeling and cell separation,^{1–5} allowing manipulation of the components that are associated with the magnetic particles by an external magnetic field. These particles are also prevalent as contrast agents for magnetic resonance imaging.^{1–5}

In order to characterize the magnetization of these particles and monitor their behavior, a sensitive detection method is required. Several techniques have been developed for detecting weak magnetic fields, for example, superconducting quantum interference devices (SQUIDs),^{6,7} giant magnetoresistive (GMR) sensors,^{8,9} vibrating sample magnetometers,^{10,11} and atomic magnetometers.¹² Magnetic resonance imaging (MRI) can also be used for diagnostics with magnetic microparticles.¹³ Each method has both advantages and disadvantages. For example, SQUIDs offer ultrahigh sensitivity and have been used extensively to detect weak magnetic signals, but they require cryogenics. GMR sensors are relatively convenient to use, however, they require the sample to be extremely close (on the order of microns) to the sensors. Vibrating sample magnetometry has relatively low sensitivity. While MRI is a powerful tool for noninvasive diagnostics, the cost of MRI machines severely limits their accessibility.

Here we explore the application of atomic magnetometry for detecting magnetic particles. Atomic magnetometry has reached sensitivity comparable to that of SQUIDs (Refs. 14 and 15) without requiring cryogenics. Details of our approach to atomic magnetometry are provided elsewhere.¹⁶ Briefly, the magnetometer is based on nonlinear (in light power) magneto-optical rotation (NMOR) of laser light interacting with rubidium atoms contained in antirelaxation coated vapor cells. The frequency of the laser light is modulated (FM), and resonances in optical rotation are observed at

modulation frequencies related to the Larmor precession frequency of the Rb atoms. The relationship between the external magnetic fields and the resonance modulation frequency ω_M is

$$\omega_M \approx 2g\mu|\mathbf{B}_{\text{bias}} + \mathbf{B}_{\text{sample}}|,$$

where g is the atomic gyromagnetic ratio and μ is the Bohr magneton, i.e., a resonance occurs when the laser-modulation frequency is twice the Larmor precession frequency of the atoms. \mathbf{B}_{bias} is an applied magnetic field that is much greater than the sample magnetic field, $\mathbf{B}_{\text{sample}}$, and so defines the detection axis. Therefore, the magnetic field from the sample along the direction of the bias field can be deduced from the frequency change of a magneto-optical resonance.

A schematic of the experimental setup is shown in Fig. 1. Two identical antirelaxation coated ^{87}Rb vapor cells inside a multilayer magnetic shield form a first-order gradiometer that is insensitive to common-mode noise from environmental fluctuations. A long piercing solenoid can be used to apply a leading field ($B_{\text{lead}} \leq 0.5 \text{ G}$) on the sample. Because of the geometry of the arrangement, the leading field is not “seen” by the magnetometer cells. A bias field of 0.7 mG (B_{bias}) gives a FM NMOR resonance frequency of $\sim 1 \text{ kHz}$ in the absence of the sample. When a magnetic sample which produces, for example, a dipole field oriented along the axis of the piercing solenoid is introduced to the detection region (the volume within the piercing solenoid in the vicinity of the sensor cells), the component of $\mathbf{B}_{\text{sample}}$ along \mathbf{B}_{bias} is of opposite sign in the two sensor cells. The signal from one arm of the gradiometer is continuously fed back to the laser modulation to keep this magnetometer on resonance. Thus the signal from the other magnetometer represents the difference field between the two cells created by the sample. We have achieved $\sim 1 \text{ nG/Hz}^{1/2}$ sensitivity for near-dc signal¹⁷ (for frequencies $\sim 0.1 \text{ Hz}$), with 1-cm-sized cells separated by 1.5 cm .

^{a)}Electronic mail: sxu@lbl.gov

^{b)}Electronic mail: pines@berkeley.edu

^{c)}Electronic mail: budker@berkeley.edu

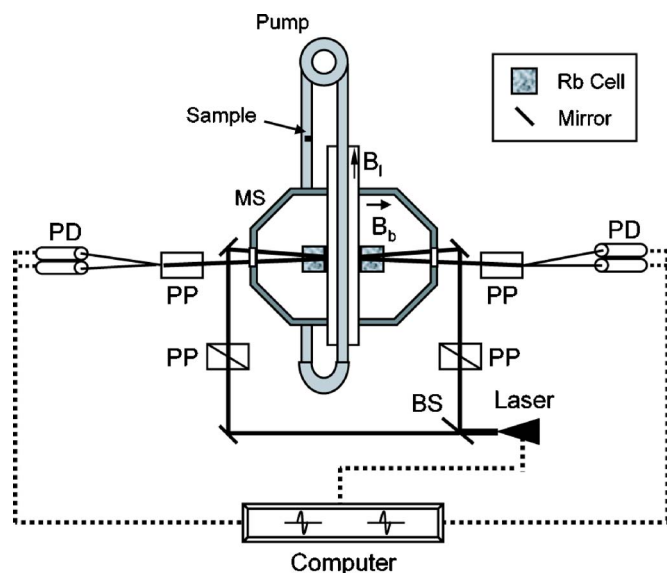


FIG. 1. (Color online) Schematic of the setup for particle detection. BS: beam splitter; PP: polarizer prism; PD: photodiode; and MS: magnetic shield.

We first measured the magnetization of a cobalt particle with an estimated diameter of $150\ \mu\text{m}$. The sample was embedded into a small piece of Styrofoam and magnetized by inserting it briefly into a 3 kG field of a permanent magnet (magnetization increased the observed signal by at least an order of magnitude). Water carrying the foam was circulated by a peristaltic pump through tubing (0.32 cm inner diameter) to the detection region of the gradiometer. As a control, an identical piece of Styrofoam without sample was also introduced into circulation. Figure 2 shows the results for two flow rates, 30 and 150 ml/min, which correspond to residence times of 160 and 30 ms, respectively, in the detection region. Each time the Styrofoam with the magnetic particle passed the gradiometer, a spikelike signal was pro-

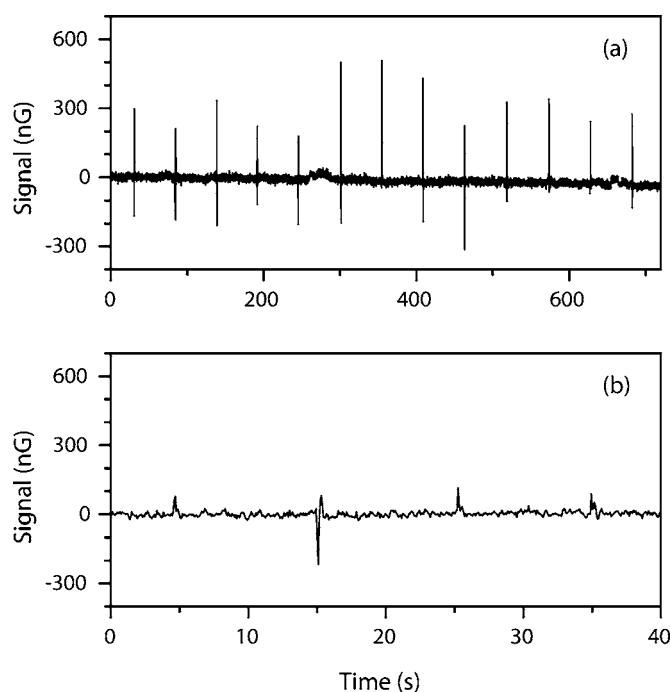


FIG. 2. Detection of a circulating cobalt particle carried by water at two different flow rates: (a) 30 ml/min and (b) 150 ml/min.

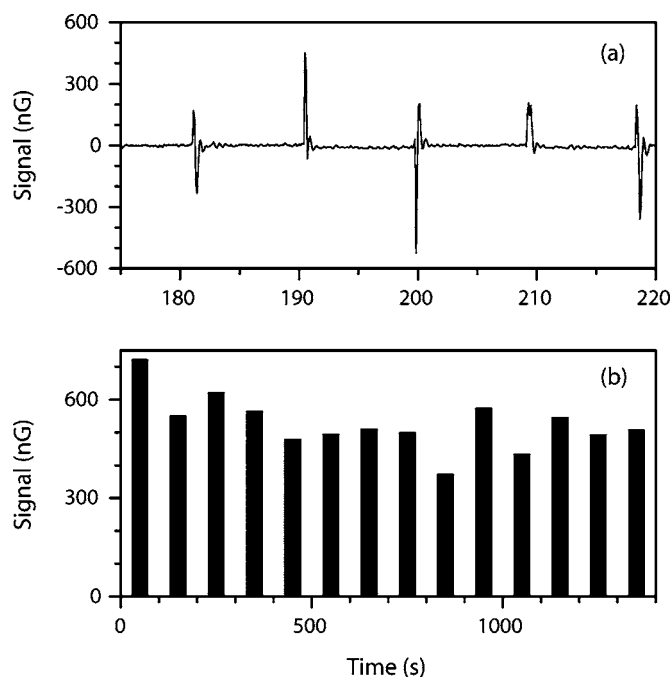


FIG. 3. Detection of 18 nl superparamagnetic magnetite suspension (4×10^5 particles): (a) typical real time detection and (b) averaged signal (peak-to-peak) of ten consecutive measurements as a function of experimental time.

duced, while the control Styrofoam produced no discernable signal. The average signal amplitude was much smaller for faster flow, since the particle spent less time in the detection region. The magnitude and time dependence of the signal fluctuated between successive detections, most likely due to the random position and orientation of the particle in the detection region. From the signal-to-noise ratio in the slower flow, we estimate the detection limit to be a single cobalt particle with $\sim 20\ \mu\text{m}$ diameter. This estimation assumes a multidomain structure of the particles and the scaling of their magnetic moment as the square root of the volume. For single-domain particles, much smaller ones can be detected. In this case, we can estimate the detection limit to be $\sim 5\ \mu\text{m}$ diameter, given the present sensitivity of the gradiometer. The throughput can be increased up to 1200 ml/min using larger-diameter tubing, with the current spacing between the two cells. Therefore, such magnetic particles can be detected at essentially arbitrarily low concentrations in a large volume, and with high throughput.

Two types of smaller particles were measured similarly. One type was a superparamagnetic suspension containing amine-coated magnetite particles with $\sim 1\ \mu\text{m}$ diameter (Sigma-Aldrich, 17643). The sample was prepared by loading 18 nl of a suspension into a piece of capillary ($150\ \mu\text{m}$ diameter, 1 mm length) and wrapping the capillary with Styrofoam. The total number of particles in the sample was $\sim 4.5 \times 10^5$. The results are shown in Fig. 3, with water flow rate of 160 ml/min. Panel (a) shows typical real time detection as the particles circulate. In order to measure the possible relaxation of the magnetization of the superparamagnetic particles, we continuously monitored the signal for over 1400 s. Averages of ten consecutive measurements are plotted versus the average measurement time after initial magnetization of the sample by a 3 kG permanent magnet [Fig. 3(b)]. (Using a 20 kG field for magnetization made no substantial difference in the signal amplitude.) No significant

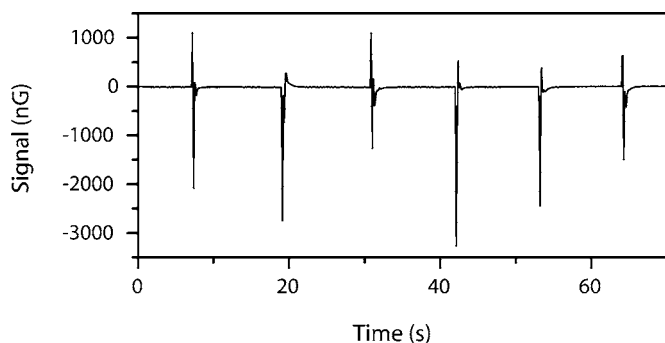


FIG. 4. Detection of 18 nl ferromagnetic fluid of cobalt nanoparticles (8.2% in kerosene).

decay was observed for the time span of the experiment. From the amplitude of the averaged signal, we estimated a detection limit of 0.2 nl, or 5×10^3 particles. The leading field was also varied between 0 and 0.5 G, which produced no observable change in the signal.

The other sample was a ferromagnetic fluid (Strem Chemicals, 27-0001) incorporating cobalt nanoparticles with diameter ~ 10 nm. The sample was loaded in a similar fashion to the superparamagnetic particles mentioned above. The ferromagnetic fluid with cobalt nanoparticles produced a strong signal because of their high magnetization (Fig. 4, water flowing at 130 ml/min). From the average signal-to-noise ratio of 360, we estimated the smallest detectable amount to be 50 pl for the fluid tested, with a detection time constant of 30 ms.

These experiments suggest diverse applications for our method. The ability to detect rare events (single particles) in a large amount of sample could be used for security applications to screen for magnetically labeled viruses in dilute environments or for in-line quality control devices for industrial processes involving magnetic products or impurities (for example, detection of ferromagnetic particulates in engine oil). Our method also has potential applications in biological and medical research. The high sensitivity could allow detection of trace amounts of proteins, DNA, or antibodies that have been labeled by magnetic beads, and in the study of biochemical events associated with the aggregation of magnetic particles.

The detection limit could be improved significantly by further optimization and modification of the apparatus. For

example, sensitivity can be improved by using additional sensor cells. A higher-order gradiometer can thus be formed, which could allow one to eliminate the need for magnetic shielding. Smaller alkali vapor cells,¹⁸ which can be put closer to the sample thus improving the sample filling factor, will also be investigated. This will enhance the detection limit, allowing the method to be coupled with microfluidic applications.

One of the authors (D.B.) acknowledges inspiration for this work from Vladimir G. Budker, and wishes to dedicate it to his memory. This work was supported by the Director of the Office of Science, Office of Basic Sciences, Materials Sciences Division of the U.S. Department of Energy, and by an ONR MURI grant.

¹Q. A. Pankhurst, J. Connolly, S. K. Jones, and J. Dobson, *J. Phys. D* **36**, R167 (2003).

²J.-M. Nam, C. S. Thaxton, and C. A. Mirkin, *Science* **301**, 1884 (2003).

³J. Connolly, T. G. St. Pierre, M. Rutnakornpituk, and J. S. Riffle, *J. Phys. D* **37**, 2475 (2004).

⁴A. K. Gupta and M. Gupta, *Biomaterials* **26**, 3995 (2005).

⁵S. Odenbach, *J. Phys.: Condens. Matter* **15**, S1497 (2003).

⁶A. Tsukamoto, K. Saitoh, D. Suzuki, N. Sugita, Y. Seki, A. Kandori, K. Tsukada, Y. Sugiura, S. Hamaoka, H. Kuma, N. Hamasaki, and K. Enpuku, *IEEE Trans. Appl. Supercond.* **15**, 656 (2005).

⁷H.-J. Krause, G. I. Panaitov, N. Wolters, D. Lomparski, W. Zander, Y. Zhang, E. Oberdoerffer, D. Wollersheim, and W. Wilke, *IEEE Trans. Appl. Supercond.* **15**, 729 (2005).

⁸D. K. Wood, K. K. Ni, D. R. Schmidt, and A. N. Cleland, *Sens. Actuators, A* **120**, 1 (2005).

⁹N. Pekas, M. D. Porter, M. Tondra, A. Popple, and A. Jander, *Appl. Phys. Lett.* **85**, 4783 (2004).

¹⁰S. M. Montemayor, L. A. García-Cerda, and J. R. Torres-Lubián, *Mater. Lett.* **59**, 1056 (2005).

¹¹P. C. Fannin, A. Slawska-Waniewska, P. Didukh, A. T. Giannitsis, and S. W. Charles, *Eur. Phys. J.: Appl. Phys.* **17**, 3 (2002).

¹²C. Affolderbach, M. Stähler, S. Knappe, and R. Wynands, *Appl. Phys. B: Lasers Opt.* **75**, 605 (2002).

¹³S. E. Turvey, E. Swart, M. C. Denis, U. Mahmood, C. Benoist, R. Weissleder, and D. Mathis, *J. Clin. Invest.* **115**, 2454 (2005).

¹⁴D. Budker, D. F. Kimball, S. M. Rochester, V. V. Yashchuk, and M. Zolotarev, *Phys. Rev. A* **62**, 043403 (2000).

¹⁵I. K. Kominis, T. W. Kornack, J. C. Allred, and M. V. Romalis, *Nature (London)* **422**, 596 (2003).

¹⁶D. Budker, D. F. Kimball, V. V. Yashchuk, and M. Zolotarev, *Phys. Rev. A* **65**, 055403 (2002).

¹⁷S. Xu, S. M. Rochester, V. V. Yashchuk, M. H. Donaldson, and D. Budker, *Rev. Sci. Instrum.* **77**, 083106 (2006).

¹⁸M. V. Balabas, D. Budker, J. Kitching, P. D. D. Schwindt, and J. E. Stalnaker, *J. Opt. Soc. Am. B* **23**, 1001 (2006).